Exact fluctuation and long-range correlations in a single-file model under resetting

Saikat Santra[1,*] and Prashant Singh[2,†]

[1]*International Centre for Theoretical Sciences, Tata Institute of Fundamental Research, Bengaluru 560089, India*

[2]*Niels Bohr International Academy, Niels Bohr Institute, University of Copenhagen, Blegdamsvej 17, 2100 Copenhagen, Denmark*

(Received 20 November 2023; accepted 24 January 2024; published 19 March 2024)

Resetting is a renewal mechanism in which a process is intermittently repeated after a random or fixed time. This simple act of stop and repeat profoundly influences the behavior of a system as exemplified by the emergence of nonequilibrium properties and expedition of search processes. Herein we explore the ramifications of stochastic resetting in the context of a single-file system called random average process (RAP) in one dimension. In particular, we focus on the dynamics of tracer particles and analytically compute the variance, equal time correlation, autocorrelation, and unequal time correlation between the positions of different tracer particles. Our study unveils that resetting gives rise to rather different behaviors depending on whether the particles move symmetrically or asymmetrically. For the asymmetric case, the system for instance exhibits a long-range correlation which is not seen in absence of the resetting. Similarly, in contrast to the reset-free RAP, the variance shows distinct scalings for symmetric and asymmetric cases. While for the symmetric case, it decays (towards its steady value) as $\sim e^{-rt}/\sqrt{t}$, we find $\sim te^{-rt}$ decay for the asymmetric case (r being the resetting rate). Finally, we examine the autocorrelation and unequal time correlation in the steady state and demonstrate that they obey interesting scaling forms at late times. All our analytical results are substantiated by extensive numerical simulations.

DOI: 10.1103/PhysRevE.109.034123

I. INTRODUCTION

Deciphering the behavior of complex systems consisting of many interacting units is a fundamental problem often encountered in statistical physics [1,2]. A classic example of an interacting particle system in nonequilibrium statistical mechanics is the single-file system, in which particles in a one-dimensional line move alongside each other, strictly obeying the constraint of nonovertaking, wherein one particle cannot pass another [3–5]. Due to this nonovertaking constraint (also referred to as single-file constraint), the dynamics of different particles become strongly correlated [6,7]. For example, in a collection of diffusing particles in one dimension with single-file constraint, the mobility of a tracer particle is drastically reduced and as a result, the mean-squared displacement grows subdiffusively as $\sim\sqrt{t}$ at late times, instead of the linear growth for a freely diffusing particle [8–11]. The coefficient of this subdiffusive growth, in turn, depends on the particle number density, the precise interaction among the particles, and the statistical properties of the initial state of the system [9,12–15]. In fact based on hydrodynamic approach, a recent work showed that this subdiffusive scaling holds true only for short-range interactions and changes to an interaction-dependent exponent for long-range interactions [16]. Beyond diffusion, such slowing down effects have also been studied for Hamiltonian systems [17–19] as well as for other stochastic systems like randomly accelerated process [20] and active processes [21–24]. In this paper we set out to study the tracer dynamics for a single-file model in the presence of a renewal mechanism called resetting that has garnered significant attention in the last decade [25].

Stochastic resetting is a simple and natural mechanism in which a dynamical process is intermittently interrupted after some random time, after which it again starts anew. A quintessential example of this phenomenon is the resetting Brownian motion, which was first studied in [25]. In this model a particle undergoing free diffusion is returned to its starting position at a certain rate r, after which it recommences diffusion until the next resetting event. As a result of this, the particle experiences an effective confinement around its initial position. However, it is important to note that this confinement arises solely from the dynamics of the system and does not stem from any physical potential. Indeed, as time progresses, the system eventually reaches a nonequilibrium steady state, which is characterized by the presence of a nonzero probability current. Another notable aspect of this model is that, unlike in free diffusion, the particle exhibits a finite mean first-passage time. Remarkably, this mean time depends nonmonotonically on the resetting rate r which indicates its optimisation for an optimal rate r^* [26]. Beyond the standard Brownian motion, resetting has also been explored within a broader spectrum of other stochastic processes [27–41] as well as in cross-disciplinary fields such as search theory [42,43], computer science [44,45], chemical and biological processes [46–49]. Furthermore, rigorous studies have been made to comprehend non-Poissonian strategies [29,50,51] and the implications of resetting in quantum settings [52–56]. On the experimental side, resetting was

*saikat.santrah@icts.res.in

†prashant.singh@nbi.ku.dk

recently realized in experiments involving a single particle in optical traps [57–59]. We refer to [41,60–63] and references therein for recent reviews on the subject.

While most of the aforementioned studies primarily focused on single-particle dynamics, there has also been a substantial surge of interest in understanding the effects of resetting for interacting particles. Examples include exclusion processes [64–67], the Ising model [68], fluctuating interfaces [69,70], and predator-prey models [71–73], among numerous others [see [62] and references therein for a review of stochastic resetting in interacting systems]. These studies investigated the scenario where multiple particles are reset *simultaneously* after a random duration (global resetting). This is contrary to some other studies where particles reset independently of the other particles (local resetting) [74–76]. In a recent work involving independently diffusing particles, but undergoing global resetting at a rate r, the authors showed that the simultaneous resetting induces a strong long-range correlation in the system [77]. Despite this correlation, the model still possesses analytical solvability based on the renewal formula, and many results on the joint probability distribution of the positions and extremal statistics were derived. Similar long-range correlation is also observed in noninteracting quantum spin system [78]. However, to the best of our knowledge, the implications of stochastic resetting on the dynamics of tracer particles in an interacting multiparticle system still remains unexplored. A natural question particularly arises: Does one still get a resetting induced long-range correlation in such interacting scenarios? In this paper we present an example of a single-file model (called the random average process) [79,80] where these questions can be thoroughly addressed through exact analytic computations.

Our system consists of a collection of particles moving in an infinite line and distributed with density ρ. We denote the position of ith particle at time t by $x_i(t)$ where $i \in \mathbb{Z}$ and $x_i(t) \in \mathbb{R}$. Initially, the particles are located at a fixed distance $a = \frac{1}{\rho}$ apart:

$$x_i(0) = ia = i/\rho, \qquad \text{for all } i \in \mathbb{Z}. \tag{1}$$

For simplicity, we take $\rho = 1$ without any loss of generality. Starting from this configuration, each particle performs the random average process interspersed by resetting events, during which the entire system is (globally) reset to the configuration in Eq. (1). This means that at any small time interval $[t, t + \Delta t]$, two events can occur: (1) either particles globally reset their positions to $x_i(0)$ in Eq. (1) with probability $r\Delta t$ or (2) they perform the random average motion with the remaining probability $(1 - r\Delta t)$. In the case of the latter event, the ith particle can jump to its right with probability $p\Delta t$ and to its left with probability $q\Delta t$. With remaining probability $[1 - (p + q)\Delta t]$, the position $x_i(t)$ does not change. The successful jump, either to the left or to the right, is by a random fraction η_i of the space available between the particle and its neighbor. This means that the jump to the right takes place by an amount $\eta_i[x_{i+1}(t) - x_i(t)]$, while to the left, the particle jumps by the amount $\eta_i[x_{i-1}(t) - x_i(t)]$. Here $\eta \in [0, 1)$ is a random variable drawn from the distribution $R(\eta)$. Notice that throughout time evolution, a particle can never overtake its neighboring particles and maintains its initial order.

The overall update rule for the position can then be written as

$$x_i(t + \Delta t) = \begin{cases} x_i(0), & \text{w.p. } r\Delta t, \\ x_i(t) + \Gamma_i(t), & \text{w.p. } (1 - r\Delta t), \end{cases} \tag{2}$$

where "w.p." stands for "with probability" and $\Gamma_i(t)$ for the increment which is given by

$$\Gamma_i(t) = \begin{cases} \eta_i[x_{i+1}(t) - x_i(t)], & \text{w.p. } p\Delta t, \\ \eta_i[x_{i-1}(t) - x_i(t)], & \text{w.p. } q\Delta t, \\ 0, & \text{w.p. } [1 - (p + q)\Delta t]. \end{cases} \tag{3}$$

Given this model, our aim in this paper is twofold. First, we aim to study the dynamics of tracer particles and explore analytically the effect of stochastic resetting on the single-file model. For this purpose, we investigate the variance and different two-point correlation functions for the positions of tracer particles. In particular, the role of resetting in the autocorrelation involving two different times so far has been studied only for a few cases such as the drift diffusion [38] and the fractional Brownian motion [39]. It also played a crucial role in income dynamics modeled using geometric Brownian motion [81]. However, all of these studies dealt with the single-particle dynamics. Here our aim is to investigate this with multiple particles and understand how fluctuations corresponding to one particle at a given time affect the position of some other particle at some later time. Second, our work will also shed light on determining whether the long-range correlation, stemming from the simultaneous resetting of noninteracting particles [77], persists even when the system involves interacting particles in its underlying dynamics.

The remainder of our paper is organized as follows: Sec. II briefly recalls the main results of the reset-free random average process. In Sec. III we illustrate the effect of resetting on the mean position of a tracer particle. These results will then be used to calculate the variance in Sec. IV A and equal time correlation in Sec. IV B. We devote Secs. V A and V B to compute, respectively, the autocorrelation and the unequal time correlation in the steady state. Finally, we conclude in Sec. VI.

II. RANDOM AVERAGE PROCESS WITHOUT RESETTING

Before we delve into discussing the consequences of resetting on tracer particles, it is instructive to review some known results for the random average process (RAP) in absence of resetting ($r = 0$). Studied originally by Fontes and Ferrari as a generalization of the smoothing process and the voter model [82], the RAP has appeared in several physical problems like force fluctuations in bead packs [83], mass transport models [84,85], models of wealth distribution and traffic [86], and the generalized Hammersley process [87]. As an interacting multiparticle system, this model is particularly interesting since the particles do not overtake each other and maintain their initial order throughout the time evolution as indicated by Eq. (2). Therefore, every particle performs the single-file motion. Due to this nonovertaking constraint, the motion of different particles get strongly correlated [79,80,88–91]. For instance, various studies based on both microscopic calculations as well as hydrodynamic approaches have shown that the

variance and the correlation of the displacement variable $z_i(t)$ [with $z_i(t) = x_i(t) - x_i(0)$] at late time is given by [80]

$$\langle z_i(t)\rangle = \mu_1(p-q)t, \tag{4}$$

$$\left\langle z_i^2(t)\right\rangle - \langle z_i(t)\rangle^2 \simeq \zeta\sqrt{t}, \tag{5}$$

$$\langle z_0(t)z_i(t)\rangle - \langle z_i(t)\rangle\langle z_0(t)\rangle \simeq \zeta\sqrt{t}\, f\left(\frac{|i|}{2\sqrt{\mu_1(p+q)t}}\right), \tag{6}$$

where the prefactor $\zeta = \mu_2\sqrt{\mu_1(p+q)}/[\sqrt{\pi}(\mu_1-\mu_2)]$ depends on first two moments μ_1 and μ_2 of the jump distribution $R(\eta)$ and the scaling function $f(y)$ in Eq. (6) is given by

$$f(y) = e^{-y^2} - \sqrt{\pi}\, y\, \mathrm{Erfc}(y). \tag{7}$$

Due to the translational symmetry in the model, both mean and variance in Eqs. (4) and (5) do not depend on the particle index i. Also the mean vanishes for the symmetric case $p = q$ since particles do not experience any drive under this condition. Meanwhile the subdiffusive scaling of the variance at large times in Eq. (5) and the scaling function $f(y)$ in Eq. (7) are hallmark properties of many single-file systems that possess diffusive hydrodynamics at the macroscopic scales [9,91].

It turns out that the variance and the correlation for single-file systems depend crucially on the statistical properties of the initial state of the system. For RAP, results in Eqs. (4)–(7) hold true only for the quenched initial condition where the initial positions are fixed to Eq. (1) for all realizations [80]. On the other hand, for annealed initial condition where initial positions are drawn from the steady state, the initial positions themselves vary from realization to realization. Under this circumstance, the variance $l_0(t)$ at late time grows as

$$l_0(t) \simeq \zeta\sqrt{2t}, \qquad \text{for } p = q, \tag{8}$$

$$\simeq \frac{\mu_1\mu_2(p-q)}{(\mu_1-\mu_2)}t, \quad \text{for } p > q. \tag{9}$$

As indicated, the temporal scaling of $l_0(t)$ depends sensitively on whether particles experience drive or not. This is contrary to the quenched case in Eq. (5) where we obtain the same scaling for both cases. Furthermore, in the case of symmetric RAP, the ratio of the variances for two cases is found to be $\sqrt{2}$, which is also observed in the context of other single-file models [9,13]. In what follows, we will investigate these quantities for nonzero r and illustrate how resetting modifies them.

III. AVERAGE POSITION

For $p \neq q$, we saw in Eq. (4) that the particles experience a net drive which gives rise to a nonzero value of mean that grows linearly with time. Let us investigate what happens to this average in presence of resetting. Here again, it turns out convenient to work in terms of the displacement variable $z_i(t) = x_i(t) - x_i(0)$ and rewrite the update rules in Eq. (2) as

$$z_i(t+\Delta t) = \begin{cases} 0, & \text{with probability } r\Delta t, \\ z_i(t)+\Gamma_i(t), & \text{with probability } (1-r\Delta t), \end{cases} \tag{10}$$

where the increment $\Gamma_i(t)$ can be written as

$$\Gamma_i(t) = \begin{cases} \eta_i[z_{i+1}(t) - z_i(t) + 1], & \text{with probability } p\Delta t, \\ \eta_i[z_{i-1}(t) - z_i(t) - 1], & \text{with probability } q\Delta t, \\ 0, & \text{with probability } 1-(p+q)\Delta t. \end{cases} \tag{11}$$

Denoting the mean as $h_i(t) = \langle z_i(t)\rangle$, we can write its evolution for a small time interval $[t, t+\Delta t]$ as

$$h_i(t+\Delta t) \simeq (1-r\Delta t)[h_i(t) + \langle\Gamma_i(t)\rangle]. \tag{12}$$

Plugging $\langle\Gamma_i(t)\rangle$ from Eq. (11) and taking $\Delta t \to 0$ limit, we obtain the following differential equation for $h_i(t)$:

$$\frac{dh_i(t)}{dt} = \mu_1[ph_{i+1}(t) + qh_{i-1}(t) - (p+q)h_i(t)] - rh_i(t) + \mu_1(p-q). \tag{13}$$

Recall that $\mu_m = \langle\eta^m\rangle = \int_0^1 d\eta\, \eta^m R(\eta)$ represents the mth moment of the jump distribution $R(\eta)$. One needs to solve this equation with the initial condition $h_i(0) = 0$. Since it is a linear equation in $h_i(t)$, we proceed to solve it by taking the Fourier transformation with respect to the index i. Defining the Fourier transformation as

$$\bar{h}(k,t) = \sum_{i=-\infty}^{\infty} h_i(t)\, e^{jik} \tag{14}$$

and the inverse Fourier transform as

$$h_i(t) = \frac{1}{2\pi}\int_{-\pi}^{\pi} dk\, \bar{h}(k,t)\, e^{-jik}, \tag{15}$$

with $j^2 = -1$, we recast Eq. (13) in terms of the Fourier variable as

$$\frac{\partial\bar{h}(k,t)}{\partial t} = -\alpha(k)\bar{h}(k,t) + 2\pi\mu_1(p-q)\delta(k), \tag{16}$$

with $\alpha(k) = r + \mu_1(p+q) - \mu_1 pe^{-jk} - \mu_1 qe^{jk}$. Finally, solving Eq. (16) and performing the inverse Fourier transformation, we get

$$h_i(t) = h(t) = \frac{\mu_1(p-q)}{r}(1-e^{-rt}). \tag{17}$$

Notice that the final expression turns out to be independent of the index i, since we have assumed translational invariance of our infinite system. Also, the mean expectedly vanishes for the symmetric $p = q$ case. Meanwhile for $r = 0$, our result reduces to Eq. (4) where the mean grows linearly with time. However, for any nonzero r, it approaches a steady value at large times. This steady value decays as $\sim 1/r$ with respect to the resetting rate. Physically, a larger resetting rate confines the tracer particle to move in the vicinity of its initial position, which gives rise to the smaller mean. In Fig. 1 we have plotted the mean $h_i(t)$ and compared it with the same obtained from numerical simulations. We observe an excellent match between them. In the following sections, we will use this expression of mean to compute different correlation functions for the tracer particles.

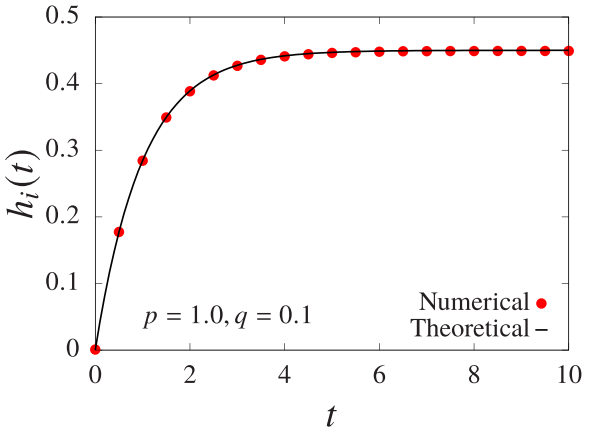

FIG. 1. Comparison of the mean $h_i(t) = \langle z_i(t)\rangle$ in Eq. (17) with the numerical simulation for $p = 1.0$, $q = 0.1$, $r = 1$, and jump distribution $R(\eta) = 1$. Simulation is conducted with $N = 101$ particles.

IV. VARIANCE AND EQUAL TIME CORRELATION

In this section we look at the variance and equal time correlations of the positions of two tagged particles when the entire system is reset to the configuration in Eq. (1) with rate r. Let us denote this correlation by $C_i(t) = \langle z_0(t) z_i(t)\rangle$. Recall that for free RAP, the correlation function satisfies a scaling behavior in $|i|/\sqrt{t}$ with the associated scaling function given in Eq. (7). Here our aim is to illustrate how this scaling behavior gets modified in presence of resetting. To this aim, we start by deriving the time evolution differential equation for $C_i(t)$. In a small time interval $[t, t+\Delta t]$, the correlation $C_i(t+\Delta t)$ for $i \neq 0$ changes by an amount

$$C_i(t+\Delta t) \simeq C_i(t) - r\Delta t\, C_i(t) + 2\mu_1(p-q)\Delta t\, h(t) + \mu_1(p+q)\Delta t[C_{i+1}(t) + C_{i-1}(t) - 2C_i(t)].$$

On the other hand, applying the same procedure for $i = 0$ gives

$$C_0(t+\Delta t) \simeq C_0(t) - r\Delta t\, C_0(t) + 2\mu_1(p-q)\Delta t\, h(t) + \mu_2(p+q)\Delta t\,\{1 + 2[C_0(t) - C_1(t)]\} + \mu_1(p+q)\Delta t[2C_1(t) - 2C_i(t)].$$

Combining both contributions for $i = 0$ and $i \neq 0$ and taking the limit $\Delta t \to 0$, we obtain

$$\frac{dC_i(t)}{dt} = \mu_1(p+q)[C_{i+1}(t) + C_{i-1}(t) - 2C_i(t)] + \delta_{i,0}\,\mu_2(p+q)\{1 + 2[C_0(t) - C_1(t)]\} + 2\mu_1(p-q)h(t) - rC_i(t). \tag{18}$$

Fortunately, this equation involves only mean and two-point correlation function and does not involve higher order correlation functions. This closure property enables us to obtain exact solution for this equation. For this, let us take the Laplace transformation with respect to t ($\to s$) as

$$\hat{C}_i(s) = \int_0^\infty dt\, e^{-st}\, C_i(t), \tag{19}$$

and rewrite Eq. (18) in terms of $\hat{C}_i(s)$ as

$$s\hat{C}_i(s) = \mu_1(p+q)[\hat{C}_{i+1}(s) + \hat{C}_{i-1}(s) - 2\hat{C}_i(s)] + \delta_{i,0}\,\mu_2(p+q)\left(\frac{1}{s} + 2[\hat{C}_0(s) - \hat{C}_1(s)]\right) - r\hat{C}_i(s) + 2\mu_1(p-q)\hat{h}(s). \tag{20}$$

While writing this equation, we have taken the initial condition $C_i(0) = 0$ and introduced the notation $\hat{h}(s)$ to denote the Laplace transformation of the mean $h(t)$, which from Eq. (17) turns out to be

$$\hat{h}(s) = \frac{\mu_1(p-q)}{r}\left(\frac{1}{s} - \frac{1}{s+r}\right). \tag{21}$$

We now proceed to solve Eq. (20). First notice that, due to the single-file constraint, we get coupling of different i in Eq. (20). To decouple them, we take the Fourier transformation

$$\mathcal{Z}(k,s) = \sum_{i=-\infty}^{\infty} \hat{C}_i(s)\, e^{jik}, \tag{22}$$

and insert this in Eq. (20) to yield

$$\mathcal{Z}(k,s) = \frac{\mu_2(p+q)\{1 + 2s[\hat{C}_0(s) - \hat{C}_1(s)]\}}{s[s + r + 2\mu_1(p+q)(1-\cos k)]} + \frac{4\pi\mu_1(p-q)\hat{h}(s)}{(s+r)}\,\delta(k). \tag{23}$$

Everything on the right-hand side is known except two functions, namely, $\hat{C}_0(s)$ and $\hat{C}_1(s)$. One of them can be expressed in terms of the other by putting $i = 0$ in Eq. (20). This results in the relation

$$\hat{C}_1(s) = \frac{[2(p+q)(\mu_1 - \mu_2) + s + r]\hat{C}_0(s)}{2(\mu_1 - \mu_2)(p+q)} - \frac{\mu_2(p+q)/s + 2\mu_1(p-q)\hat{h}(s)}{2(\mu_1 - \mu_2)(p+q)}, \tag{24}$$

which we substitute in Eq. (23) to yield

$$\mathcal{Z}(k,s) = \frac{\mu_2}{s}\frac{\mu_1(p+q) - s(s+r)\hat{C}_0(s) + 2\mu_1 s(p-q)\hat{h}(s)}{(\mu_1 - \mu_2)[s + r + 2\mu_1(p+q)(1-\cos k)]} + \frac{4\pi\mu_1(p-q)\hat{h}(s)}{(s+r)}\,\delta(k). \tag{25}$$

We now have only one unknown $\hat{C}_0(s)$. However, this can be computed self-consistently as shown later. Finally inverting $\mathcal{Z}(k,s)$ in k gives the exact correlation as

$$\hat{C}_i(s) = \frac{2\mu_1(p-q)\hat{h}(s)}{s+r} + \hat{\mathcal{G}}_i(s), \tag{26}$$

where the function $\hat{\mathcal{G}}_i(s)$ is defined as

$$\hat{\mathcal{G}}_i(s) = \frac{\mu_2[\mu_1(p+q) - s(s+r)\,\hat{\mathcal{G}}_0(s)]}{s(\mu_1 - \mu_2)}\mathcal{V}_i(s+r), \tag{27}$$

$$\mathcal{V}_i(s) = \frac{1}{2\pi}\int_{-\pi}^{\pi} dk\, \frac{e^{-jik}}{s + 2\mu_1'(1-\cos k)}, = \frac{1}{\sqrt{s^2 + 4\mu_1' s}}\left(\frac{s + 2\mu_1' - \sqrt{s^2 + 4\mu_1' s}}{2\mu_1'}\right)^{|i|} \tag{28}$$

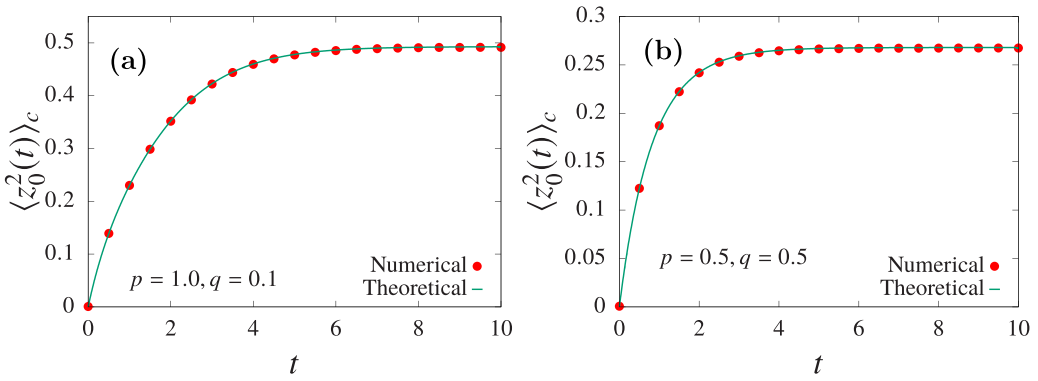

FIG. 2. Comparison of $\langle z_0^2(t)\rangle_c$ in Eq. (33) with the numerical simulation for two sets of parameters: $p = 1.0$, $q = 0.1$ in panel (a) and $p = 0.5$, $q = 0.5$ in panel (b). For both panels, we have performed simulation with $N = 101$ particles, resetting rate $r = 1$, and jump distribution $R(\eta) = 1$.

with $\mu_1' = \mu_1(p+q)$. To summarize, we have calculated the exact two-point correlation functions in Eq. (26) in terms of the Laplace variable s. The idea now is to perform the inversion and obtain them in the time domain. For simplicity, we carry out this inversion separately for the $i = 0$ and $i \neq 0$ cases below.

A. Variance of $z_0(t)$

We first look at the variance for which we put $i = 0$ in Eq. (26). Looking at this expression, it is clear that one needs to invert the Laplace transformation $\hat{\mathcal{G}}_0(s)$. We rewrite its expression from Eq. (27) as

$$\hat{\mathcal{G}}_0(s) = \frac{\mu_1\mu_2(p+q)(\mu_1-\mu_2)^{-1}(s\sqrt{s+r})^{-1}}{\left[\sqrt{(s+r)+4\mu_1(p+q)} + \frac{\mu_2}{\mu_1-\mu_2}\sqrt{s+r}\right]}. \quad (29)$$

Fortunately, one can perform this inversion exactly, and we show in Appendix A that

$$\mathcal{G}_0(t) = \frac{\mu_2(\mu_1-\mu_2)(p+q)}{\sqrt{r}(\mu_1-2\mu_2)} \times \int_0^t dT\, e^{-rT}\, \mathrm{Erf}[\sqrt{r(t-T)}]Z(T), \quad (30)$$

where $\mathcal{G}_0(t)$ stands for the Laplace transformation of $\hat{\mathcal{G}}_0(s)$ and the function $Z(t)$ is defined as

$$Z(t) = \frac{1}{\sqrt{\pi t}}\left(e^{-4\mu_1 t(p+q)} - \frac{\mu_2}{\mu_1-\mu_2}\right) - \frac{\mu_2}{\mu_2-\mu_2}\sqrt{-B_1}\, e^{-B_1 t}\, \mathrm{Erf}(\sqrt{-B_1 t}) + \sqrt{-B_2}\, e^{-B_1 t}\, \mathrm{Erf}(\sqrt{-B_2 t}). \quad (31)$$

Constants B_1 and B_2 depend on the model parameters as $B_1 = 4(p+q)(\mu_1-\mu_2)^2/(\mu_1-2\mu_2)$ and $B_2 = B_1 - 4\mu_1(p+q)$. Finally, using Eq. (30) in Eq. (26), we obtain

$$C_0(t) = \mathcal{G}_0(t) + \frac{2\mu_1^2(p-q)^2}{r^2}[1-e^{-rt}(rt+1)], \quad (32)$$

from which the variance of $z_0(t)$ turns out to be

$$\langle z_0^2(t)\rangle_c = C_0(t) - \langle z_0(t)\rangle^2, = \mathcal{G}_0(t) + \frac{\mu_1^2(p-q)^2}{r^2}[1-e^{-rt}(2rt+e^{-rt})]. \quad (33)$$

This represents the exact variance of the position of a tagged particle in RAP with resetting. Figure 2 illustrates the comparison of our analytical results with the numerical simulations for both symmetric and asymmetric cases. An excellent match is seen in both cases. For any nonzero r, we anticipate the expression in Eq. (33) to attain a stationary value at large times. To show this, one can, in principle, directly put $t \to \infty$ in Eq. (30) and carry out the integration. However, it turns out more convenient to put $s \to 0$ limit in $\hat{\mathcal{G}}_0(s)$ and use the formula $\mathcal{G}_0(t \to \infty) = \lim_{s\to 0}[s\hat{\mathcal{G}}_0(s)]$. With this procedure, the stationary value of the variance turns out to be

$$\langle z_0^2(t\to\infty)\rangle_c = \frac{\mu_1^2(p-q)^2}{r^2} + \frac{\mu_1\mu_2(p+q)}{\sqrt{r}(\mu_1-\mu_2)} \times \left[\sqrt{r+4\mu_1(p+q)} + \frac{\mu_2\sqrt{r}}{\mu_1-\mu_2}\right]^{-1}. \quad (34)$$

Recall that for $r = 0$, the tracer particle does not attain any stationary value. This indicates that the stationary value of the variance should diverge as $r \to 0$. From the exact expression in Eq. (34), we find that $\langle z_0^2(t\to\infty)\rangle_c$ diverges differently depending on whether the particles move symmetrically ($p = q$) or asymmetrically ($p \neq q$). For $p = q$, the stationary value diverges as $\sim r^{-1/2}$ as $r \to 0$, whereas for $p \neq q$, it diverges as $\sim r^{-2}$. Contrarily for large r, $\langle z_0^2(t\to\infty)\rangle_c$ decays as $\sim 1/r$ for both cases.

After analyzing the stationary value of the variance, let us look at its time-dependent form in Eq. (33). While this is an exact expression, it has rather a complicated form. To gain some insights into it, we will analyze it for large t and study the relaxation properties. For continuity of presentation, we have shown this calculation in Appendix A and quote only the final result here. We find $d(t) = \langle z_0^2(t\to\infty)\rangle_c - \langle z_0^2(t)\rangle_c$ is

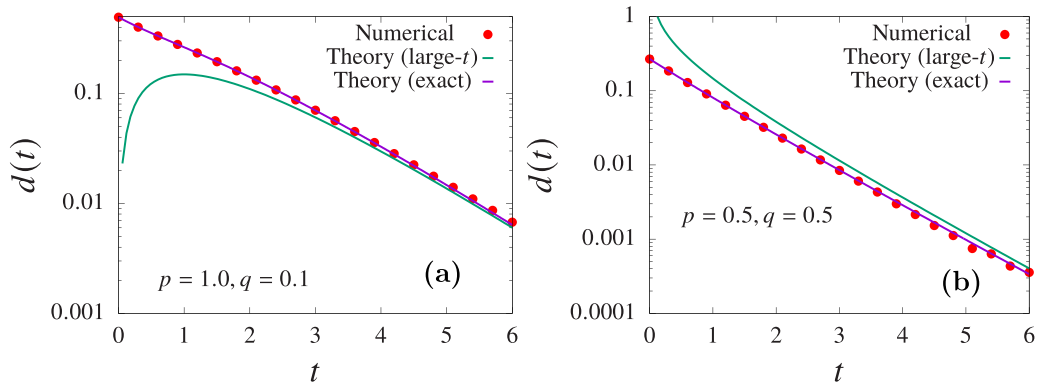

FIG. 3. Comparison of the relaxation behavior of the variance $\langle z_0^2(t)\rangle_c$ for the symmetric ($p = q$) and asymmetric ($p \neq q$) cases. For illustration, we have plotted $d(t) = \langle z_0^2(t \to \infty)\rangle_c - \langle z_0^2(t)\rangle_c$ in Eq. (36) and compared it with the numerical simulation for two sets of parameters: $p = 1.0$, $q = 0.1$ in panel (a) and $p = q = 0.5$ in panel (b). For both panels, we have performed simulation with $N = 101$ particles, resetting rate $r = 1$ and jump distribution $R(\eta) = 1$.

given by

$$d(t) \simeq \frac{\mu_2\sqrt{\mu_1 p}}{\sqrt{2\pi} r(\mu_1 - \mu_2)} \frac{e^{-rt}}{\sqrt{t}}, \quad \text{for } p = q, \tag{35}$$

$$\simeq \frac{2\mu_1^2(p-q)^2}{r^2} rt e^{-rt}, \quad \text{for } p \neq q. \tag{36}$$

Interestingly, we find different relaxation behaviors depending on whether $p = q$ or $p \neq q$. While for the symmetric case, the variance relaxes as $\sim e^{-rt}/\sqrt{t}$ to its stationary value, we obtain $\sim te^{-rt}$ relaxation for the asymmetric case. Note that such a difference between the symmetric and the asymmetric variances is not seen for free RAP ($r = 0$), and we obtain the same subdiffusive scaling for both cases as shown in Eq. (5). Indeed, writing the time evolution equation for the variance $\langle z_0^2(t)\rangle_c$ for the free RAP, one can show that it can be made independent of p and q by suitably scaling $t \to (p+q)t$ [80]. Therefore, we get same temporal scaling of the variance for both symmetric and the asymmetric cases. However, in the presence of resetting, we get an additional timescale in the problem ($\sim 1/r$) and the time evolution equation cannot be rendered independent of p and q. This gives rise to different behaviors for two cases. This key difference is one of the consequences of the resetting. In Fig. 3 we have compared the relaxation properties with the numerical simulations for $p = q$ case [Fig. 3(b)] and $p \neq q$ case [Fig. 3(a)]. We observe an excellent agreement between our theory and numerics for both cases.

B. Correlation $C_i(t) = \langle z_0(t) z_i(t)\rangle$ for $i \neq 0$

After analyzing the variance of the position of a tagged particle, let us now look at the position correlation for two different tagged particles. For free RAP, we saw in Eq. (6) that the two-point correlation function satisfies nontrivial scaling behavior in $\sim |i|/\sqrt{t}$ with i being the separation between two particles. The associated scaling function is given in Eq. (7). In this section we study the correlation function in presence of resetting and calculate $C_i(t) = \langle z_0(t) z_i(t)\rangle$ for $i \neq 0$. Its expression in the Laplace domain is given in Eq. (26) from which it is clear that we have to perform the inverse Laplace transformation of $\hat{\mathcal{G}}_i(s)$. Rewriting its expression from Eq. (27),

$$\hat{\mathcal{G}}_i(s) = \hat{\mathcal{G}}_0(s) \times \hat{w}_i(s + r), \tag{37}$$

$$\text{with } \hat{w}_i(s) = \left(\frac{s + 2\mu_1' - \sqrt{s^2 + 4\mu_1' s}}{2\mu_1'} \right)^{|i|}, \tag{38}$$

where we have defined $\mu_1' = \mu_1(p+q)$. In order to perform the inverse Laplace transformation of $\hat{\mathcal{G}}_i(s)$, we have to carry out two inversions: one is for $\hat{\mathcal{G}}_0(s)$ and the other is for $\hat{w}_i(s)$. Now, for $\hat{\mathcal{G}}_0(s)$, we have already computed this inversion in Eq. (30). On the other hand, for $\hat{w}_i(s)$, its inversion in the time domain [denoted by $w_i(t)$] is given by [92]

$$w_i(t) = \frac{|i|}{t} e^{-2\mu_1' t} I_{|i|}(2\mu_1' t), \quad \text{for } i \neq 0. \tag{39}$$

Finally using the convolution form of $\hat{\mathcal{G}}_i(s)$ in Eq. (37) gives

$$\mathcal{G}_i(t) = \int_0^t dT\, e^{-rT}\, w_i(T)\, \mathcal{G}_0(t - T). \tag{40}$$

inserting which in Eq. (26), we obtain

$$C_i(t) = \int_0^t dT\, e^{-rt}\, w_i(T)\, \mathcal{G}_0(t - T) + \frac{2\mu_1^2(p-q)^2}{r^2}[1 - e^{-rt}(rt + 1)]. \tag{41}$$

Remember that $C_i(t) = \langle z_0(t) z_i(t)\rangle$, and in order to obtain the connected correlation, we subtract the mean contributions as follows:

$$\langle z_0(t) z_i(t)\rangle_c = \langle z_0(t) z_i(t)\rangle - \langle z_0(t)\rangle\langle z_i(t)\rangle,$$
$$= \int_0^t dT\, e^{-rt}\, w_i(T)\, \mathcal{G}_0(t - T) + \frac{\mu_1^2(p-q)^2}{r^2}[1 - e^{-rt}(2rt + e^{-rt})]. \tag{42}$$

It is worth mentioning that even for free RAP, only asymptotic results for $\langle z_0(t) z_i(t)\rangle_c$ are known [80]. Our analysis here provides an exact expression for the correlation valid for all

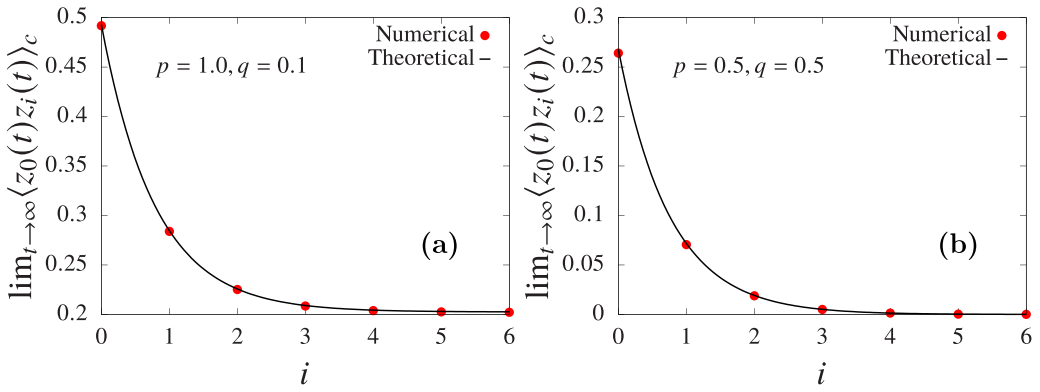

FIG. 4. Comparison of the equal time correlation $\langle z_0(t)z_i(t)\rangle_c$ in the steady state ($t \to \infty$) in Eq. (44) for for two sets of parameters: $p = 1.0$, $q = 0.1$ in panel (a) and $p = 0.5$, $q = 0.5$ in panel (b). In both panels, simulation has been carried out with $N = 101$ particles, resetting rate $r = 1$, and jump distribution $R(\eta) = 1$.

times and not just at large times. However, at large times, one can simplify this expression. In fact, putting $t \to \infty$ in Eq. (40), one can see that

$$\mathcal{G}_i(t \to \infty) = \mathcal{G}_0(t \to \infty)\, \hat{w}_i(r), \tag{43}$$

where the steady value $\mathcal{G}_0(t \to \infty)$ is given in Eq. (A14) and $\hat{w}_i(r)$ is given in Eq. (38). Using these expressions, we find that the correlation between two tracer particles in the steady state is given by

$$\langle z_0(t)z_i(t)\rangle_c \overset{t\to\infty}{=} \mathcal{G}_0^{\rm st} \exp\left(-\frac{|i|}{\xi_p}\right) + \frac{\mu_1^2(p-q)^2}{r^2}, \tag{44}$$

where $\mathcal{G}_0^{\rm st} = \mathcal{G}_0(t \to \infty)$ is defined in Eq. (A14) and the decay length ξ_p is defined as

$$\xi_p = |\log\left(r + 2\mu_1' - \sqrt{r^2 + 4\mu_1' r}\right) - \log(2\mu_1')|^{-1}. \tag{45}$$

Interestingly for $p \neq q$, we find that the correlation decays to a nonzero constant value as $|i| \to \infty$. Contrarily, it decays to zero for $p = q$. For reset-free RAP, this correlation decays to zero both for the symmetric and the asymmetric cases. Our study unravels that resetting affects these two cases in different manners and manifestly gives rise to long-range correlations only for the $p \neq q$ case. Recently, resetting induced long-range correlation was also found in independently diffusing particles but subjected to simultaneous resetting at a rate r [77]. Here we have extended this result for interacting single-file systems. Physically, the long-range correlation can be understood as follows: Consider two particles with positions $x_0(t)$ and $x_l(t)$ with $l \gg 1$. Both these particles experience an effective attraction around their initial positions due to the resetting event. However, this attraction has a purely dynamical interpretation and does not arise due to any physical potential. Furthermore, for $p > q$, all particles that lie between $x_0(t)$ and $x_l(t)$ experience a net drift towards $x_l(t)$. As a result of this combined effect of attraction and drift, the positions $x_0(t)$ and $x_l(t)$ of two particles become strongly correlated. Figure 4 shows the comparison of our analytical results with the same obtained using numerical simulation. Indeed, even in simulations, we find that the correlation $C_i(t)$ does not decay to zero for the asymmetric case.

V. UNEQUAL TIME CORRELATIONS

So far we have presented rigorous results on the variance and the equal time correlation and demonstrated how resetting modifies these quantities. Our analysis showed that contrary to the reset-free RAP model, these quantities, in the presence of resetting, behave differently depending on the presence or absence of drive in the dynamics. Continuing with this, we now look at the autocorrelation and the unequal time position correlations for two tracer particles. Let us denote this correlation by $S_i(t_0, t_0 + t) = \langle z_0(t_0)z_i(t_0 + t)\rangle$. As done before, we again consider a small time interval $[t_0 + t, t_0 + t + dt]$ and follow the update rules in Eqs. (10) and (11) to write the total change in $S_i(t_0, t_0 + t)$ within this interval. This results in the following differential equation:

$$\frac{dS_i(t_0, t_0 + t)}{dt} = -rS_i + \mu_1(p - q)h(t_0) + \mu_1[pS_{i+1} + qS_{i-1} - (p + q)S_i]. \tag{46}$$

Solving this equation by taking the joint Fourier-Laplace transformations as

$$\tilde{S}(k, t_0, t_0 + t) = \sum_{i=-\infty}^{\infty} e^{jik}\, S_i(t_0, t_0 + t), \tag{47}$$

$$\mathbb{S}(k, s, t) = \int_0^{\infty} dt_0\, e^{-st_0}\, \tilde{S}(k, t_0, t_0 + t), \tag{48}$$

and inserting them in Eq. (46), we obtain

$$\frac{d\mathbb{S}}{dt} = -\alpha(k)\mathbb{S} + 2\pi\mu_1(p - q)\hat{h}(s)\delta(k), \tag{49}$$

where $\alpha(k) = r + \mu_1(p + q) - \mu_1 pe^{-jk} - \mu_1 qe^{jk}$. Since we are interested in computing the correlations in the steady state (i.e., $t_0 \to \infty$), we will analyze Eq. (49) in the small-s limit. In Appendix B, we have explicitly carried out this analysis

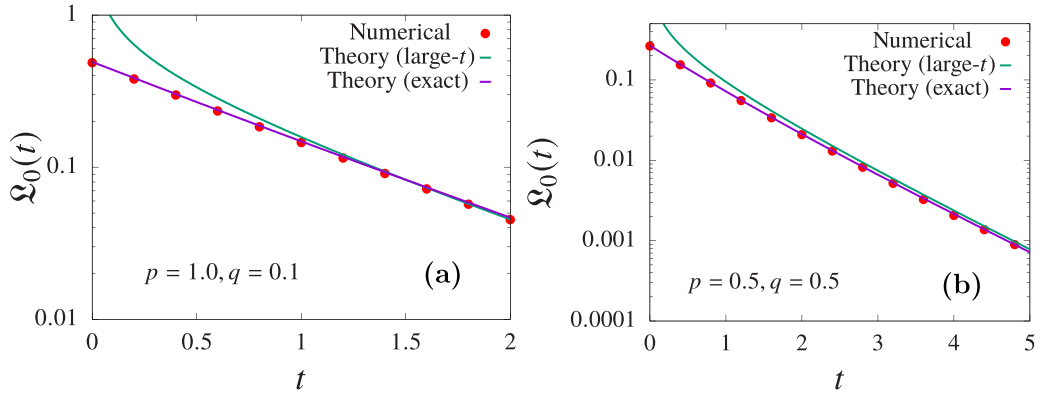

FIG. 5. Autocorrelation $\mathcal{L}_0(t)$ has been compared with the numerical simulations for $p = 1.0, q = 0.1$ in panel (a) and $p = 0.5, q = 0.5$ in panel (b). We have plotted both the exact expression in Eq. (52) as well as the asymptotic (large-t) expression in Eq. (54). Simulation has been performed with $N = 101$ particles, resetting rate $r = 1$, and jump distribution $R(\eta) = 1$.

and obtained the correlation $S_i(t_0, t_0 + t)$ measured from the steady state ($t_0 \to \infty$) as

$$S_i(t_0, t_0 + t) \simeq \frac{\mathcal{B}r}{2\pi}\int_{-\pi}^{\pi} dk\, \frac{e^{-jik-\alpha(k)t}}{r + 2\mu_1'(1-\cos k)} + \frac{\mu_1^2(p-q)^2}{r^2}(1 + e^{-rt}) \tag{50}$$

$$\text{with}\quad \mathcal{B} = \sqrt{\frac{r + 4\mu_1'}{r}}\,\mathcal{G}_0^{\rm st}, \tag{51}$$

where again we have used the notation $\mu_1' = \mu_1(p+q)$ and $\mathcal{G}_0^{\rm st} = \mathcal{G}_0(t_0 \to \infty)$ is defined in Eq. (A14). Subtracting the mean contribution from this correlation, we obtain the connected correlation $\mathcal{L}_i(t)$ as

$$\mathcal{L}_i(t) = [S_i(t_0, t_0 + t) - \langle z_0(t_0)\rangle\,\langle z_i(t_0 + t)\rangle]_{t_0\to\infty},$$
$$= \frac{\mathcal{B}r}{2\pi}\int_{-\pi}^{\pi} dk\, \frac{e^{-jik-\alpha(k)t}}{r + 2\mu_1'(1-\cos k)} + \frac{\mu_1^2(p-q)^2}{r^2}e^{-rt}. \tag{52}$$

For $t = 0$, one can perform the integration over k, and the result matches with the equal time correlation in Eq. (44) in the steady state. On the other hand, for nonzero t, performing this integration turns out to be difficult. However, for large t, we could carry out the integration rigorously and obtain some asymptotic results. Below we discuss this first for the autocorrelation ($i = 0$) and then for general i.

A. Autocorrelation $\mathcal{L}_0(t)$

To get large t-behavior of $\mathcal{L}_0(t)$, we first notice that one gets exponentially decaying terms like $\sim\exp[-2\mu_1(p+q)t\,\sin^2(k/2)]$ inside the integration in Eq. (52). For large t, such integrations will be dominated by smaller values of k. Therefore, performing small-k approximation in Eq. (52), we get

$$\mathcal{L}_0(t) \simeq \frac{\mathcal{B}e^{-rt}}{2\pi}\int_{-\pi}^{\pi} dk\, e^{-jk\mu_1(p-q)t - \mu_1 t(p+q)k^2/2} + \frac{\mu_1^2(p-q)^2}{r^2}e^{-rt}. \tag{53}$$

Next, we change the variable $u = k\sqrt{\mu_1(p+q)t}$ in this equation and carry out the integration for large t to obtain

$$\mathcal{L}_0(t) \simeq \frac{\mathcal{B}\,e^{-\left[r + \frac{\mu_1(p-q)^2}{2(p+q)}\right]t}}{\sqrt{2\pi\mu_1(p+q)t}} + \frac{\mu_1^2(p-q)^2}{r^2}e^{-rt}. \tag{54}$$

Using this expression, we again find that the large time decay of $\mathcal{L}_0(t)$ depends on whether the particles experience a drift or not. While for the symmetric case, the autocorrelation in the steady state decays as $\sim e^{-rt}/\sqrt{t}$ at late times, we observe an exponential decay $\sim e^{-rt}$ for the asymmetric ($p \neq q$) case. This is contrary to the case of simple resetting Brownian motion, where autocorrelation in the steady state decays exponentially as e^{-rt} at all times [38,39]. However, for interacting particles, $\mathcal{L}_0(t)$ has a more complicated form and picks up exponential decay (or otherwise) only at large times. In Fig. 5 we have compared this late time decay with the numerical simulations. We observe that while the simulation data deviate from Eq. (54) at small times, the agreement becomes better at larger times.

B. Unequal time correlation $\mathcal{L}_i(t)$

We now analyze Eq. (52) for general i. For this case also we can perform the small-k approximation in Eq. (52) for larger values of t since the integral has exponentially decaying terms like $\sim\exp[-2\mu_1(p+q)t\,\sin^2(k/2)]$. We then obtain

$$\mathcal{L}_i(t) \simeq \frac{\mathcal{B}e^{-rt}}{2\pi}\int_{-\pi}^{\pi} dk\, e^{-jik - jk\mu_1(p-q)t - \mu_1 t(p+q)k^2/2} + \frac{\mu_1^2(p-q)^2}{r^2}e^{-rt}. \tag{55}$$

To perform the integration over k, we change the variable $u = k\sqrt{\mu_1(p+q)t}$ and plug it into this equation. Finally, we find that the $\mathcal{L}_i(t)$ satisfies the scaling relation

$$\mathcal{L}_i(t) - \mathcal{L}_{|i|\to\infty}(t) \simeq \frac{\mathcal{B}\,e^{-rt}}{\sqrt{2\pi\mu_1(p+q)t}}\,\mathcal{M}\left[\frac{i + \mu_1(p-q)t}{\sqrt{2\mu_1(p+q)t}}\right], \tag{56}$$

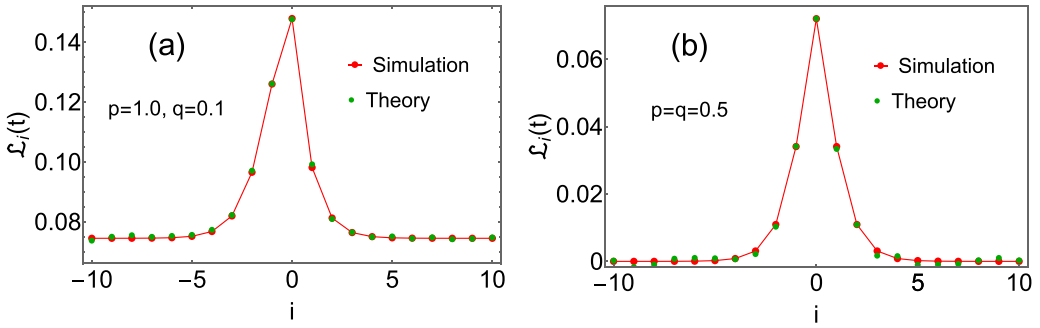

FIG. 6. Unequal time correlation $\mathcal{L}_i(t)$ in Eq. (52) is compared with the numerical simulation for asymmetric ($p > q$) RAP in the left panel and symmetric ($p = q$) RAP in the right panel for $t = 1$. Parameters chosen are $r = 1$, $R(\eta) = 1$ and number of particles $N = 101$ for simulation.

where the scaling functions $\mathcal{M}(y)$ and $\mathcal{L}_{|i|\to\infty}(t)$ are given by

$$\mathcal{M}(y) = e^{-y^2} \text{ and } \mathcal{L}_{|i|\to\infty}(t) = \frac{\mu_1^2(p-q)^2}{r^2} e^{-rt}. \quad (57)$$

Note that this scaling behavior is entirely an outcome of the resetting dynamics and does not appear for the reset-free RAP [80]. Looking at Eq. (56), once again we see that for the asymmetric RAP, $\mathcal{L}_i(t)$ takes a nonzero value as $|i| \to \infty$ indicating a long-range correlation between two particles. However, this value decays exponentially with time, and as $t \to \infty$, this long-range correlation vanishes. As discussed in the case of equal time correlation, the appearance of long-range correlation turns out to be an interplay of the effective attraction experienced by the particles around their resetting sites and a net drift due to asymmetric rates.

In Fig. 6 we have compared the exact expression of $\mathcal{L}_i(t)$ in Eq. (52) with the numerical simulations for $p \neq q$ in Fig. 6(a) and $p = q$ in Fig. 6(b). For both cases, we see an excellent agreement between theory and numerics. However, demonstrating the scaling behavior of $\mathcal{L}_i(t)$ in Eq. (56) in simulation turns out to be difficult. It turns out that one needs to go to very large values of t in order to observe this scaling relation. For instance, in Fig. 7 we see that this scaling behavior becomes valid at around $t = 200$. However, the value of $\mathcal{L}_i(t)$ at such large times is very small due to the presence $\sim e^{-rt}$ term in Eq. (56). Measuring such small values in simulation is difficult. Therefore, to validate this scaling relation, we have plotted the exact $\mathcal{L}_i(t)$ in Fig. 7 for different values of t by numerically performing the integration over k. At large t, we recover the scaling function $\mathcal{M}(y)$ (see Fig. 7).

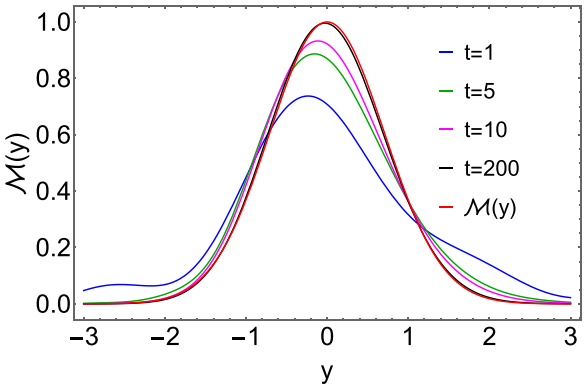

FIG. 7. Scaling function $\mathcal{M}(y)$ in Eq. (56) for the unequal time correlation $\mathcal{L}_i(t)$ is compared with the exact expression of $\mathcal{L}_i(t)$ in Eq. (52) for different values of t and $p = 1.0$, $q = 0.1$, $r = 1$, and jump distribution $R(\eta) = 1$.

VI. CONCLUSION

In conclusion we have studied the motion of tracer particles in a one-dimensional single-file model called the random average process which is subjected to stochastic resetting. The resetting mechanism, characterized by a constant rate r, causes the entire system being reinstated to the configuration given in Eq. (1). Utilizing an exact microscopic analysis, we calculated key statistical quantities such as variance, equal time correlation, autocorrelation, and unequal time correlation for the positions of tracer particles. Through these calculations, we demonstrated how resetting modifies the system and gives rise to properties which are otherwise not observed in absence of the resetting

We first looked at the variance $\langle z_0^2(t)\rangle_c$ whose exact expression is given in Eq. (33). At large times, it expectedly attains a stationary value given in Eq. (34). To gain some physical insights, we further explored the relaxation behavior of $\langle z_0^2(t)\rangle_c$ as it approaches its stationary value. Interestingly, this relaxation process turns out to crucially depend on whether the particles move symmetrically ($p = q$) or asymmetrically ($p \neq q$) on either side. While for the symmetric case, the variance relaxes as $\sim e^{-rt}/\sqrt{t}$ to its stationary value, we obtain $\sim te^{-rt}$ relaxation for the asymmetric case. Note that such a difference between the symmetric and the asymmetric variances is not seen for free RAP ($r = 0$), and we obtain the same subdiffusive scaling for both cases as shown in Eq. (5). Resetting introduces an additional timescale in the model which leads to different behaviors for two cases. This key difference is one of the consequences of the resetting.

We next turned our attention to the equal time position correlation for two different tracer particles. Focusing on the steady state, our study revealed that resetting induces a long-range correlation only for the asymmetric case. On the other hand, for the symmetric case, we obtained correlations that

decay exponentially with the distance in Eq. (44). In a recent work involving independently diffusing particles, but undergoing global resetting at a rate r, the authors showed that the simultaneous resetting induces a strong long-range correlation in the system [77]. Our work generalizes these results in the interacting single-file setup and shows that simultaneous resetting induces a long-range correlation only when particles experience a bias ($p \neq q$).

Finally, we investigated the autocorrelation and the unequal time position correlation in the steady state. For the autocorrelation $\mathcal{L}_0(t)$, once again, we find that the large-t decay is different for $p = q$ and $p \neq q$ cases. Specifically, for the symmetric case $\mathcal{L}_0(t)$ exhibited a decay of $\sim e^{-rt}/\sqrt{t}$, while for the asymmetric case, the decay followed $\mathcal{L}_0(t) \sim e^{-rt}$. Conversely, the unequal time position correlation $\mathcal{L}_i(t)$ exhibits a scaling behavior in terms of the variable $y = [i + \mu_1(p - q)t]/\sqrt{t}$. The associated scaling function $\mathcal{M}(y)$ is written in Eq. (57). We emphasize that this scaling behavior is entirely an outcome of the resetting dynamics and does not appear for the reset-free RAP [80].

Studying analytically an interacting multiparticle system is difficult because of the correlation between different particles. Here we presented a specific single-file model for which exact microscopic computations can be carried out. Our work pointed to a crucial difference in the tracer dynamics for symmetric RAP and asymmetric RAP, both subjected to resetting at a rate r. For future direction, it would be interesting to explore an intermediate case where only some of the particles experience bias while all others move symmetrically [88,89] and see if one still gets a resetting induced long-range correlation. Also, our paper focused on one specific model of single-file motion called the random average process. It remains a promising direction to study effects of resetting on other single-file models like single-file diffusion [8–11], in active particles [21–24,93–95], and in experiments [57–59]. Furthermore, throughout our paper, we have focused on the global resetting mechanism where all particles are simultaneously reset to their initial positions. This choice is also consistent with typical experimental setups where the resetting mechanism is implemented via global confining potentials that pull particles towards their minimum [57–59]. Therefore while global resetting seemed natural to us, we also emphasize that exploring tracer dynamics with other resetting mechanisms (like partially resetting, local resetting [74–76]) in multiparticle systems remains an important future direction. Finally, we have only looked at different two-point correlation functions in our paper. Obtaining higher moments and the distribution function for the position of a tracer particle still remains an open problem even for the reset-free RAP.

ACKNOWLEDGMENTS

We thank Arnab Pal and R. K. Singh for their useful comments on the paper. S.S. acknowledges the support of the Department of Atomic Energy, Government of India, under Project No. 19P1112&D. P.S. acknowledges the support of the Novo Nordisk Foundation under the Grant No. NNF21OC0071284.

APPENDIX A: DERIVATION OF THE VARIANCE $\langle z_0^2(t)\rangle_c$ IN EQ. (33)

In this Appendix we provide a detailed derivation of the variance $\langle z_0^2(t)\rangle_c = \langle z_0^2(t)\rangle - \langle z_0(t)\rangle^2$ in Eq. (33). The starting point is to find $C_0(t) = \langle z_0^2(t)\rangle$ for which we need the Laplace transform $\hat{C}_0(s)$ in Eq. (26). We rewrite this expression here as

$$\hat{C}_0(s) = \frac{2\mu_1^2(p-q)^2}{s(s+r)^2} + \hat{\mathcal{G}}_0(s), \tag{A1}$$

with $\hat{\mathcal{G}}_0(s)$ defined as

$$\hat{\mathcal{G}}_0(s) = \frac{\mu_2(\mu_1-\mu_2)(p+q)}{(\mu_1-2\mu_2)}\hat{H}(s)\hat{Z}(s+r), \quad \text{with}$$
$$\hat{Z}(s) = \frac{\sqrt{s+4\mu_1(p+q)} - \frac{\mu_2}{\mu_1-\mu_2}\sqrt{s}}{s + \frac{4(p+q)(\mu_1-\mu_2)^2}{\mu_1-2\mu_2}} \text{ and}$$
$$\hat{H}(s) = \frac{1}{s\sqrt{s+r}}. \tag{A2}$$

To evaluate the first term in the right-hand side of Eq. (A1), we use the relation

$$\int_0^\infty dt\, e^{-st}\left[\frac{1-e^{-rt}(rt+1)}{r^2}\right] = \frac{1}{s(s+r)^2}. \tag{A3}$$

On the other hand, for the second term, we use the convolution structure of $\hat{\mathcal{G}}_0(s)$, which gives $\mathcal{G}_0(t)$ as

$$\mathcal{G}_0(t) = \frac{\mu_2(\mu_1-\mu_2)(p+q)}{(\mu_1-2\mu_2)}\int_0^t dT\, e^{-rT}\, H(t-T)\, Z(T). \tag{A4}$$

Here $H(t)$ and $Z(t)$ are inverse Laplace transforms of $\hat{H}(s)$ and $\hat{Z}(s)$, respectively. Using *Mathematica*, we find $H(t) = \mathrm{Erf}(\sqrt{rt})/\sqrt{r}$ and $Z(t)$ as

$$Z(t) = \frac{1}{\sqrt{\pi t}}\left(e^{-4\mu_1 t(p+q)} - \frac{\mu_2}{\mu_1-\mu_2}\right) - \frac{\mu_2}{\mu_2-\mu_2}\sqrt{-B_1}\, e^{-B_1 t}\,\mathrm{Erf}(\sqrt{-B_1 t}) + \sqrt{-B_2}\, e^{-B_1 t}\,\mathrm{Erf}(\sqrt{-B_2 t}), \tag{A5}$$

with $B_1 = 4(p+q)(\mu_1-\mu_2)^2/(\mu_1-2\mu_2)$ and $B_2 = B_1 - 4\mu_1(p+q)$. Substituting these expressions in Eq. (A4) yields

$$\mathcal{G}_0(t) = \frac{\mu_2(\mu_1-\mu_2)(p+q)}{\sqrt{r}(\mu_1-2\mu_2)}\int_0^t dT\, e^{-rT} \times \mathrm{Erf}[\sqrt{r(t-T)}]\, Z(T). \tag{A6}$$

We now have both terms from the right-hand side of Eq. (A1). Performing the inverse Laplace transformation, we get

$$C_0(t) = \mathcal{G}_0(t) + \frac{2\mu_1^2(p-q)^2}{r^2}[1-e^{-rt}(rt+1)], \tag{A7}$$

from which the variance of $z_0(t)$ turns out to be

$$\langle z_0^2(t)\rangle_c = C_0(t) - \langle z_0(t)\rangle^2, = \mathcal{G}_0(t) + \frac{\mu_1^2(p-q)^2}{r^2}[1-e^{-rt}(2rt+e^{-rt})], \tag{A8}$$

with $\mathcal{G}_0(t)$ given in Eq. (A6). This expression of $\langle z_0^2(t)\rangle_c$ is quoted in Eq. (33).

Let us now analyze this expression to extract the asymptotic behavior of the variance. To perform the integration in Eq. (A6), we substitute the error function for large t as

$$\mathrm{Erf}(\sqrt{r(t-T)}) \simeq 1 - \frac{e^{-r(t-T)}}{\sqrt{\pi r(t-T)}} \tag{A9}$$

and plug it into Eq. (A6) as

$$\mathcal{G}_0(t) \simeq \frac{\mu_2(\mu_1-\mu_2)(p+q)}{\sqrt{r}(\mu_1-2\mu_2)}\Big[\int_0^t dT\, e^{-rT} Z(T) - \frac{e^{-rt}}{\sqrt{\pi r}}\int_0^t dT\, \frac{Z(T)}{\sqrt{t-T}}\Big].$$

For $t\to\infty$, the first term inside the bracket $[\cdot]$ simply becomes the Laplace transform $\hat{Z}(r)$ in Eq. (A2). Therefore, one can recast $\mathcal{G}_0(t)$ as

$$\mathcal{G}_0(t) \simeq \frac{\mu_2(\mu_1-\mu_2)(p+q)}{\sqrt{r}(\mu_1-2\mu_2)}\Big[\hat{Z}(r) - \frac{e^{-rt}}{\sqrt{\pi r}}\int_0^t dT\, \frac{Z(T)}{\sqrt{t-T}}\Big]. \tag{A10}$$

Next, we have to evaluate the integral over T for larger values of t. Defining $J(t) = \int_0^t dT\, \frac{Z(T)}{\sqrt{t-T}}$, we take its Laplace transform with respect to t ($\to s$) as

$$\hat{J}(s) = \sqrt{\frac{\pi}{s}}\,\hat{Z}(s). \tag{A11}$$

We take the small-s limit of this equation, which corresponds to its large-t limit in the time domain

$$\hat{J}(s\to 0) \simeq \frac{(\mu_1-2\mu_2)\sqrt{\mu_1}}{\sqrt{4(p+q)}(\mu_1-\mu_2)^2}\sqrt{\frac{\pi}{s}}. \tag{A12}$$

Now performing the inverse Laplace transformation, we obtain

$$J(t) \simeq \frac{(\mu_1-2\mu_2)\sqrt{\mu_1}}{\sqrt{4(p+q)t}(\mu_1-\mu_2)^2}, \quad \text{as } t\to\infty. \tag{A13}$$

Using this in Eq. (A10), we obtain

$$\mathcal{G}_0(t) \simeq \frac{\mu_1\mu_2(p+q)}{\sqrt{r}(\mu_1-\mu_2)}\Big[\sqrt{r+4\mu_1(p+q)} + \frac{\mu_2\sqrt{r}}{\mu_1-\mu_2}\Big]^{-1} - \frac{\mu_1\sqrt{\mu_1(p+q)}}{2r(\mu_1-\mu_2)}\,\frac{e^{-rt}}{\sqrt{\pi t}}, \tag{A14}$$

and plugging this into Eq. (A8) gives the relaxation behavior of $\langle z_0^2(t)\rangle_c$ in Eqs. (35) and (36).

APPENDIX B: UNEQUAL TIME CORRELATION $S_i(t_0, t_0+t)$ IN THE STEADY STATE ($t_0\to\infty$)

This Appendix provides a derivation of the unequal time correlation $S_i(t_0, t_0+t)$ in Eq. (50). Let us first denote by $\mathbb{S}(k,s,t)$ the joint Fourier-Laplace transform of $S_i(t_0,t_0+t)$ [see Eq. (48)]. We showed in Eq. (49) that $\mathbb{S}(k,s,t)$ satisfies the differential equation

$$\frac{d\mathbb{S}(k,s,t)}{dt} = -\alpha(k)\mathbb{S}(k,s,t) + 2\pi\mu_1(p-q)\hat{h}(s)\delta(k), \tag{B1}$$

where $\alpha(k) = r + \mu_1(p+q) - \mu_1 p e^{jk} - \mu_1 q e^{-jk}$. Solving this equation with the initial condition $\mathbb{S}(k,s,t=0) = \mathcal{Z}(k,s)$ in Eq. (25) gives

$$\mathbb{S}(k,s,t) = \mathcal{Z}(k,s)\,e^{-\alpha(k)t} + 2\pi\hat{h}(s)h(t). \tag{B2}$$

Since we are interested in finding the correlation at the steady state (i.e., $t_0\to\infty$), we analyze Eq. (B2) in the small-s limit. For $\hat{h}(s)$, we use Eq. (21) to obtain $\hat{h}(s\to 0) \simeq \mu_1(p-q)/rs$. On the other hand, using Eq. (25), we find $\mathcal{Z}(k,s)$ as

$$\mathcal{Z}(k,s\to 0) \simeq \frac{\mathcal{B}r}{s[r+2\mu_1(p+q)(1-\cos k)]} + \frac{4\pi\mu_1^2(p-q)^2}{r^2 s}\,\delta(k), \tag{B3}$$

where $\mathcal{B}$ is a constant that depends on model parameters and is given in Eq. (51). Finally plugging Eq. (B3) in $\mathbb{S}(k,s,t)$ in Eq. (B2) and performing the inverse Fourier transformation, we find

$$S_i(t_0,t_0+t)|_{t_0\to\infty} = \frac{1}{2\pi}\int_{-\pi}^{\pi} dk\, e^{-jik}\, s\,\mathbb{S}(k,s,t)|_{s\to 0}, \tag{B4}$$

$$= \frac{\mathcal{B}r}{2\pi}\int_{-\pi}^{\pi} dk\, \frac{e^{-jik-\alpha(k)t}}{r+2\mu_1(p+q)(1-\cos k)} + \frac{\mu_1^2(p-q)^2}{r^2}(1+e^{-rt}). \tag{B5}$$

This result is quoted in Eq. (50).

[1] E. H. Lieb and D. C. Mattis, *Mathematical Physics in One Dimension: Exactly Solvable Models of Interacting Particles* (Academic Press, New York, 1966).

[2] V. Privman, *Nonequilibrium Statistical Mechanics in One Dimension* (Cambridge University Press, 1997).

[3] T. E. Harris, Diffusion with collisions between particles, J. Appl. Probab. **2**, 323 (1965).

[4] D. W. Jepsen, Dynamics of a simple many-body system of hard rods, J. Math. Phys. **6**, 405 (1965).

[5] R. Arratia, The motion of a tagged particle in the simple symmetric exclusion system on Z, Ann. Probab. **11**, 362 (1983).

[6] A. Poncet, A. Grabsch, P. Illien, and O. Bénichou, Generalized correlation profiles in single-file systems, Phys. Rev. Lett. **127**, 220601 (2021).

[7] A. Grabsch, P. Rizkallah, A. Poncet, P. Illien, and O. Bénichou, Exact spatial correlations in single-file diffusion, Phys. Rev. E **107**, 044131 (2023).

[8] P. L. Krapivsky, K. Mallick, and T. Sadhu, Dynamical properties of single-file diffusion, J. Stat. Mech.: Theory Exp. (2015) P09007.

[9] P. L. Krapivsky, K. Mallick, and T. Sadhu, Large deviations in single-file diffusion, Phys. Rev. Lett. **113**, 078101 (2014).

[10] O. Bénichou, P. Illien, G. Oshanin, A. Sarracino, and R. Voituriez, Tracer diffusion in crowded narrow channels, J. Phys.: Condens. Matter **30**, 443001 (2018).
[11] S. Alexander and P. Pincus, Diffusion of labeled particles on one-dimensional chains, Phys. Rev. B **18**, 2011 (1978).
[12] P. L. Krapivsky, K. Mallick, and T. Sadhu, Tagged particle in single-file diffusion, J. Stat. Phys. **160**, 885 (2015).
[13] T. Banerjee, R. L. Jack, and M. E. Cates, Role of initial conditions in one-dimensional diffusive systems: Compressibility, hyperuniformity, and long-term memory, Phys. Rev. E **106**, L062101 (2022).
[14] E. Barkai and R. Silbey, Theory of single file diffusion in a force field, Phys. Rev. Lett. **102**, 050602 (2009).
[15] N. Leibovich and E. Barkai, Everlasting effect of initial conditions on single-file diffusion, Phys. Rev. E **88**, 032107 (2013).
[16] R. Dandekar, P. L. Krapivsky, and K. Mallick, Dynamical fluctuations in the Riesz gas, Phys. Rev. E **107**, 044129 (2023).
[17] C. Hegde, S. Sabhapandit, and A. Dhar, Universal large deviations for the tagged particle in single-file motion, Phys. Rev. Lett. **113**, 120601 (2014).
[18] A. Roy, O. Narayan, A. Dhar, and S. Sabhapandit, Tagged particle diffusion in one-dimensional gas with Hamiltonian dynamics, J. Stat. Phys. **150**, 851 (2013).
[19] M. Kollmann, Single-file diffusion of atomic and colloidal systems: Asymptotic laws, Phys. Rev. Lett. **90**, 180602 (2003).
[20] T. W. Burkhardt, Tagged-particle statistics in single-file motion with random-acceleration and Langevin dynamics, J. Stat. Phys. **177**, 806 (2019).
[21] E. Teomy and R. Metzler, Transport in exclusion processes with one-step memory: Density dependence and optimal acceleration, J. Phys. A: Math. Theor. **52**, 385001 (2019).
[22] M. Galanti, D. Fanelli, and F. Piazza, Persistent random walk with exclusion, Eur. Phys. J. B **86**, 456 (2013).
[23] P. Dolai, A. Das, A. Kundu, C. Dasgupta, A. Dhar, and K. V. Kumar, Universal scaling in active single-file dynamics, Soft Matter **16**, 7077 (2020).
[24] T. Banerjee, R. L. Jack, and M. E. Cates, Tracer dynamics in one dimensional gases of active or passive particles, J. Stat. Mech.: Theory Exp. (2022) 013209.
[25] M. R. Evans and S. N. Majumdar, Diffusion with stochastic resetting, Phys. Rev. Lett. **106**, 160601 (2011).
[26] M. R. Evans and S. N. Majumdar, Diffusion with optimal resetting, J. Phys. A: Math. Theor. **44**, 435001 (2011).
[27] S. N. Majumdar, S. Sabhapandit, and G. Schehr, Dynamical transition in the temporal relaxation of stochastic processes under resetting, Phys. Rev. E **91**, 052131 (2015).
[28] A. Pal, Diffusion in a potential landscape with stochastic resetting, Phys. Rev. E **91**, 012113 (2015).
[29] A. Pal and S. Reuveni, First passage under restart, Phys. Rev. Lett. **118**, 030603 (2017).
[30] L. Kusmierz, S. N. Majumdar, S. Sabhapandit, and G. Schehr, First order transition for the optimal search time of Lévy flights with resetting, Phys. Rev. Lett. **113**, 220602 (2014).
[31] P. C. Bressloff, Directed intermittent search with stochastic resetting, J. Phys. A: Math. Theor. **53**, 105001 (2020).
[32] S. Reuveni, Optimal stochastic restart renders fluctuations in first passage times universal, Phys. Rev. Lett. **116**, 170601 (2016).
[33] D. Gupta, Stochastic resetting in underdamped Brownian motion, J. Stat. Mech.: Theory Exp. (2019) 033212.
[34] P. Singh, Random acceleration process under stochastic resetting, J. Phys. A: Math. Theor. **53**, 405005 (2020).
[35] M. R. Evans and S. N. Majumdar, Run and tumble particle under resetting: A renewal approach, J. Phys. A: Math. Theor. **51**, 475003 (2018).
[36] V. Kumar, O. Sadekar, and U. Basu, Active Brownian motion in two dimensions under stochastic resetting, Phys. Rev. E **102**, 052129 (2020).
[37] P. Singh and A. Pal, Extremal statistics for stochastic resetting systems, Phys. Rev. E **103**, 052119 (2021).
[38] V. Stojkoski, T. Sandev, L. Kocarev, and A. Pal, Autocorrelation functions and ergodicity in diffusion with stochastic resetting, J. Phys. A: Math. Theor. **55**, 104003 (2022).
[39] S. N. Majumdar and G. Oshanin, Spectral content of fractional Brownian motion with stochastic reset, J. Phys. A: Math. Theor. **51**, 435001 (2018).
[40] P. Singh and A. Pal, First-passage Brownian functionals with stochastic resetting, J. Phys. A: Math. Theor. **55**, 234001 (2022).
[41] A. Pal, S. Kostinski, and S. Reuveni, The inspection paradox in stochastic resetting, J. Phys. A: Math. Theor. **55**, 021001 (2022).
[42] A. Pal, L. Kuśmierz, and S. Reuveni, Search with home returns provides advantage under high uncertainty, Phys. Rev. Res. **2**, 043174 (2020).
[43] A. Montanari and R. Zecchina, Optimizing searches via rare events, Phys. Rev. Lett. **88**, 178701 (2002).
[44] M. Luby, A. Sinclair, and D. Zuckerman, Optimal speedup of las vegas algorithms, Inf. Proc. Lett. **47**, 173 (1993).
[45] P. Hamlin, W. J. Thrasher, W. Keyrouz, and M. Mascagni, Geometry entrapment in walk-on-subdomains, Monte Carlo Methods Appl. **25**, 329 (2019).
[46] S. Reuveni, M. Urbakh, and J. Klafter, Role of substrate unbinding in Michaelis–Menten enzymatic reactions, Proc. Natl. Acad. Sci. USA **111**, 4391 (2014).
[47] E. Roldán, A. Lisica, D. Sánchez-Taltavull, and S. W. Grill, Stochastic resetting in backtrack recovery by RNA polymerases, Phys. Rev. E **93**, 062411 (2016).
[48] P. C. Bressloff, Modeling active cellular transport as a directed search process with stochastic resetting and delays, J. Phys. A: Math. Theor. **53**, 355001 (2020).
[49] A. Pal, S. Reuveni, and S. Rahav, Thermodynamic uncertainty relation for first-passage times on Markov chains, Phys. Rev. Res. **3**, L032034 (2021).
[50] A. Nagar and S. Gupta, Diffusion with stochastic resetting at power-law times, Phys. Rev. E **93**, 060102(R) (2016).
[51] A. Chechkin and I. M. Sokolov, Random search with resetting: A unified renewal approach, Phys. Rev. Lett. **121**, 050601 (2018).
[52] B. Mukherjee, K. Sengupta, and S. N. Majumdar, Quantum dynamics with stochastic reset, Phys. Rev. B **98**, 104309 (2018).
[53] M. Kulkarni and S. N. Majumdar, Generating entanglement by quantum resetting, Phys. Rev. A **108**, 062210 (2023).
[54] R. Yin and E. Barkai, Restart expedites quantum walk hitting times, Phys. Rev. Lett. **130**, 050802 (2023).
[55] R. Yin and E. Barkai, Instability in the quantum restart problem, arXiv:2301.06100.
[56] V. Dubey, R. Chetrite, and A. Dhar, Quantum resetting in continuous measurement induced dynamics of a qubit, J. Phys. A: Math. Theor. **56**, 154001 (2023).

[57] O. Tal-Friedman, A. Pal, A. Sekhon, S. Reuveni, and Y. Roichman, Experimental realization of diffusion with stochastic resetting, J. Phys. Chem. Lett. **11**, 7350 (2020).
[58] B. Besga, A. Bovon, A. Petrosyan, S. N. Majumdar, and S. Ciliberto, Optimal mean first-passage time for a Brownian searcher subjected to resetting: Experimental and theoretical results, Phys. Rev. Res. **2**, 032029(R) (2020).
[59] B. Besga, F. Faisant, A. Petrosyan, S. Ciliberto, and S. N. Majumdar, Dynamical phase transition in the first-passage probability of a Brownian motion, Phys. Rev. E **104**, L012102 (2021).
[60] M. R. Evans, S. N. Majumdar, and G. Schehr, Stochastic resetting and applications, J. Phys. A: Math. Theor. **53**, 193001 (2020).
[61] S. Gupta and A. M. Jayannavar, Stochastic resetting: A (very) brief review, Front. Phys. **10**, 789097 (2022).
[62] A. Nagar and S. Gupta, Stochastic resetting in interacting particle systems: A review, J. Phys. A: Math. Theor. **56**, 283001 (2023).
[63] A. Pal, V. Stojkoski, and T. Sandev, Random resetting in search problems, arXiv:2310.12057.
[64] U. Basu, A. Kundu, and A. Pal, Symmetric exclusion process under stochastic resetting, Phys. Rev. E **100**, 032136 (2019).
[65] O. Sadekar and U. Basu, Zero-current nonequilibrium state in symmetric exclusion process with dichotomous stochastic resetting, J. Stat. Mech.: Theory Exp. (2020) 073209.
[66] S. Karthika and A. Nagar, Totally asymmetric simple exclusion process with resetting, J. Phys. A: Math. Theor. **53**, 115003 (2020).
[67] S. Mishra and U. Basu, Symmetric exclusion process under stochastic power-law resetting, J. Stat. Mech.: Theory Exp. (2023) 053202.
[68] M. Magoni, S. N. Majumdar, and G. Schehr, Ising model with stochastic resetting, Phys. Rev. Res. **2**, 033182 (2020).
[69] S. Gupta, S. N. Majumdar, and G. Schehr, Fluctuating interfaces subject to stochastic resetting, Phys. Rev. Lett. **112**, 220601 (2014).
[70] S. Gupta and A. Nagar, Resetting of fluctuating interfaces at power-law times, J. Phys. A: Math. Theor. **49**, 445001 (2016).
[71] G. Mercado-Vásquez and D. Boyer, Lotka–Volterra systems with stochastic resetting, J. Phys. A: Math. Theor. **51**, 405601 (2018).
[72] M. R. Evans, S. N. Majumdar, and G. Schehr, An exactly solvable predator prey model with resetting, J. Phys. A: Math. Theor. **55**, 274005 (2022).
[73] R. K. Singh and S. Singh, Capture of a diffusing lamb by a diffusing lion when both return home, Phys. Rev. E **106**, 064118 (2022).
[74] P. L. Krapivsky, O. Vilk, and B. Meerson, Competition in a system of Brownian particles: Encouraging achievers, Phys. Rev. E **106**, 034125 (2022).
[75] A. Miron and S. Reuveni, Diffusion with local resetting and exclusion, Phys. Rev. Res. **3**, L012023 (2021).
[76] A. Pelizzola, M. Pretti, and M. Zamparo, Simple exclusion processes with local resetting, Europhys. Lett. **133**, 60003 (2021).
[77] M. Biroli, H. Larralde, S. N. Majumdar, and G. Schehr, Extreme statistics and spacing distribution in a Brownian gas correlated by resetting, Phys. Rev. Lett. **130**, 207101 (2023).
[78] M. Magoni, F. Carollo, G. Perfetto, and I. Lesanovsky, Emergent quantum correlations and collective behavior in non-interacting quantum systems subject to stochastic resetting, Phys. Rev. A **106**, 052210 (2022).
[79] G. M. Schütz, Exact tracer diffusion coefficient in the asymmetric random average process, J. Stat. Phys. **99**, 1045 (2000).
[80] R. Rajesh and S. N. Majumdar, Exact tagged particle correlations in the random average process, Phys. Rev. E **64**, 036103 (2001).
[81] V. Stojkoski, P. Jolakoski, A. Pal, T. Sandev, L. Kocarev, and R. Metzler, Income inequality and mobility in geometric Brownian motion with stochastic resetting: Theoretical results and empirical evidence of non-ergodicity, Philos. Trans. R. Soc. A **380**, 20210157 (2022).
[82] P. Ferrari and L. Fontes, Fluctuations of a surface submitted to a random average process, Electron. J. Probab. **3**, 1 (1998).
[83] S. N. Coppersmith, C.-h. Liu, S. Majumdar, O. Narayan, and T. A. Witten, Model for force fluctuations in bead packs, Phys. Rev. E **53**, 4673 (1996).
[84] R. Rajesh and S. N. Majumdar, Conserved mass models and particle systems in one dimension, J. Stat. Phys. **99**, 943 (2000).
[85] J. Krug and J. Garcia, Asymmetric particle systems on R, J. Stat. Phys. **99**, 31 (2000).
[86] S. Ispolatov, P. L. Krapivsky, and S. Redner, Wealth distributions in asset exchange models, Eur. Phys. J. B **2**, 267 (1998).
[87] D. Aldous and P. Diaconis, Hammersley's interacting particle process and longest increasing subsequences, Probab. Theor. Rel. Fields **103**, 199 (1995).
[88] J. Cividini, A. Kundu, S. N. Majumdar, and D. Mukamel, Exact gap statistics for the random average process on a ring with a tracer, J. Phys. A: Math. Theor. **49**, 085002 (2016).
[89] A. Kundu and J. Cividini, Exact correlations in a single-file system with a driven tracer, Europhys. Lett. **115**, 54003 (2016).
[90] J. Cividini, A. Kundu, S. N. Majumdar, and D. Mukamel, Correlation and fluctuation in a random average process on an infinite line with a driven tracer, J. Stat. Mech.: Theory Exp. (2016) 053212.
[91] J. Cividini and A. Kundu, Tagged particle in single-file diffusion with arbitrary initial conditions, J. Stat. Mech.: Theory Exp. (2017) 083203.
[92] H. Bateman and B. M. Project, *Tables of Integral Transforms* (McGraw-Hill, New York, 2023).
[93] P. Singh and A. Kundu, Crossover behaviours exhibited by fluctuations and correlations in a chain of active particles, J. Phys. A: Math. Theor. **54**, 305001 (2021).
[94] S. Put, J. Berx, and C. Vanderzande, Non-Gaussian anomalous dynamics in systems of interacting run-and-tumble particles, J. Stat. Mech.: Theory Exp. (2019) 123205.
[95] S. Santra, P. Singh, and A. Kundu, Tracer dynamics in active random average process, arXiv:2307.09908.